COMPARATIVE EXPERIMENTAL RESEARCH AND ANALYSIS ON SHRINKAGE & CREEP IN PRESTRESSED CONCRETE MEMBERS

Di Hu, School of Civil Engineering and Architecture, Central South University, China.
Zhengqing Chen, School of Civil Engineering, Hunan University, China.

ABSTRACT

Eight prestressed concrete T-section beams, six meters in length, constructed with high strength concrete (HSC50) and high performance concrete (HPC50) were designed to compare their characteristics of shrinkage, creep and camber. Several conclusions have been drawn from comparative test over 600 days, and some aspects on controlling camber of prestressed concrete members are discussed. The newly established formulae, based on restraint influence coefficient of steel to creep and shrinkage effect, can be easily used to calculate time-dependent effect in prestressed concrete members. These formulae accept steel ratio, steel arrangement, steel relaxation and sectional character of concrete. Results of theoretical analysis agree reasonably well with the measured test data. The reliable experimental data will be useful to engineering design and theoretical analysis.

Keywords: Prestressed concrete member, High performance concrete, Shrinkage, Creep, Restraint influence coefficient

INTRODUCTION

At any cross sections of prestressed concrete members, as we know, the stresses between concrete, prestressed steel and nonprestressed steel will be redistributed due to combined effect of creep and shrinkage of concrete and relaxation of prestressed steel; in general, the def- lection also will be increased if the resultant of forces at sections is not an axial force which exists commonly in practical members. Thus, how to predict accurate time-dependent stress redistribution and deflection, and then to control the deflection in a limited value is very important in some cases, e.g., for non-ballast prestressed concrete bridges commonly adopted in highspeed railway which show great advantages both in performance and economy by avoiding the serious problem that the ballast is easy to be powderized due to dynamic. Because high smooth-going is required by train and the permitted adjustment of the rail fas- tener is very limited, controlling the long-term deflection becomes one of the most impor -tant key techniques whether the non-ballast prestressed concrete bridges can be used successfully in highspeed railway. As china is engaging in developing highspeed railway at pre- sent and a numerous of non-ballast prestressed concrete bridges will be built, how to predict accurately long-term deflection of bridges and restrict it in a permissible value holds practical significance.

Three effective approaches can be adopted to control long-term deflection: renewing mixture design, innovative structural design and refining construction techniques. Renewing mixture design means either optimizing proportional ratio to reduce the creep and shrinkage such as lowering the content of water while selecting suitable coarse aggregate, or adding new admixture to form new kinds of concrete with much higher performance along with low creep and shrinkage which we can call high performance concrete. From the point of view of structural design, one of the most effective methods is to lower the difference of stresses between top fiber and bottom fiber in section which essentially leads to deflection. As to construction, postponing to build bridge deck pavement and accessory structures after stretching steels (self-weight of beam begins to act automatically) will reduce creep and incremental deflection greatly, for the rate of creep slows down as age of concrete increases.

Based on above discussion while taking into account sectional stress state and load history in practical bridges, eight concrete T-section beams with six meters long, constructed with high strength concrete (HSC) and high performance concrete (HPC) respectively, are designed to compare their behavior of creep, shrinkage, camber, and the restraint of steel to them. As most superstructure of prestressed concrete bridge in china at present is designed for a compressive strength from 40MPa to 55MPa, 50MPa compressive strength is designed purposely for both HSC and HPC which we can denote HSC50 and HPC50, respectively.

The main purpose of this paper is to present and discuss the results of comparative experiment and to provide simple but satisfied accurate formulae, based on the concept of restraint influence coefficient of steel to creep and shrinkage, to calculate the time-dependent stress, strain and deflection. Formulae accept steel relaxation, steel ratio, steel arrangement and sectional shape of concrete.

COMPONENTS, MIXTURE RATIO DESIGN AND MECHANICAL BEHAVIOR OF CONCRETE

Two commonly used coarse aggregates, crushed limestone and gravel, are adopted to produce HSC50 and HPC50, respectively, to compare their characteristics of creep under the same condition. Experimental resultant shows that HSC50 with crushed limestone has almost the same characteristics as that of HSC50 with gravel, while HPC50 with crushed limestone has much lower creep than HPC50 with gravel (value of creep of the former is approximately 60 percent of the latter for 60 days load duration), so crushed limestone is used to fabricate HSC50 and HPC50. Mixture ratio and properties are presented in Table 1, mechanical behavior of hardened concrete is presented in Table 2.

Table 1 Mixture Ratio and Mixture Behavior of Concrete

Mixture Ratio (kg/m^3)							Mixture Behavior	
	C	UFAC	S	G	W	TQN	slump(mm)	density(kg/m^3)
HSC	500	—	600	1160	175	3.75	125	2500
HPC	300	200	620	1190	165	3.75	100	2450

Table 2 Mechanical Behavior of Concrete

Standard Curing (20℃)						（Unit: MPa）	
	$f_{cu,3}$	$f_{cu,10}$	$f_{cu,28}$	$f_{cp,10}$	$f_{cp,28}$	$E_{10}(\times 10^3)$	$E_{28}(\times 10^3)$
HSC	46.6	62.4	69.2	55.3	58.1	42.7	47.6
HPC	44.1	62.0	69.2	57.2	62.3	47.1	47.6

Experimental results show that replacing 40 percent of Portland cement in HPC50 with UFAC composed of fly ash and slag has no obvious effect on mechanical behavior comparing to HSC50, ratio of tension to compression of HPC50 is from 1/10 to 1/12.

BEAM FABRICAION, MEASURE SYSTEM AND MAIN DESIGN PARAMETERS

Eight T-section beams are divided into two groups, in which B1 ~ B4 are made of HSC-50 and B5 ~ B8 are made of HPC50. All beams have the same dimension and nonprestressed

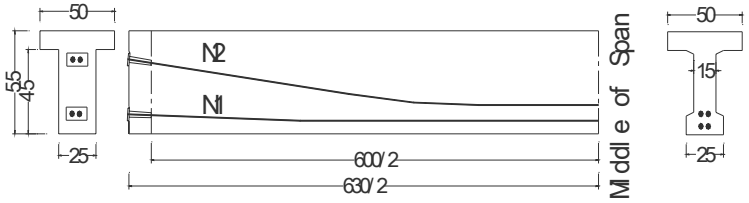

Fig.1 Beam Model (Unit:cm)

steel arrangement (Fig.1) while prestressed steel are applied only to B2 ~ B4 and B6 ~ B8, for B1 and B5 are designed to measure free shrinkage including the effect of temperature and humidity.

Imitating sectional stress state and load history of practical bridges, steels are stretched after ten days ($t_0 = 10d$) of wet curing, and first extra load 7.7KN/M is added over beam at the same time.Two months ($t_1 = 70d$) later second extra load 9.33KN/M is added over beam.

In order to guarantee the reliance of measurement, both electric measure system and mechanical measure system are adopted to ensure correctness of results by comparing and checking their data in each reading. Three vibrating-wire strain gauges, embedded into mid-span section (Fig.2a), can provide strain and temperature simultaneously. Mechanical gauges (Fig.2b) are arranged symmetrically at two sides along the beam to measure vertical displacement and longitudinal strain at midspan.Main design parameters are listed in Table 3.

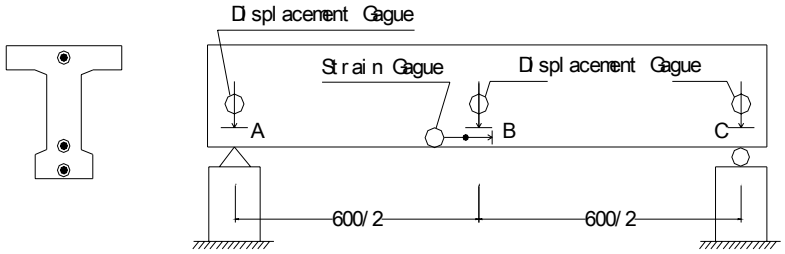

Fig.2 Arrangement of Measure Points (Unit:cm)

Table 3 Main Design Parameters of Beam

Parameters	**Unit**	**Value**	**Noticification**
Sectional Area of Concrete (Ac)	M^2	0.123	Midspan
Second Moment of Area (Ic)	M^4	0.004	Midspan
Distance from centroid of concrete to centroid of steel (e)	M	0.2105	Midspan
Area of Prestressed Steel (A_p)	M^2	0.0005576	Midspan
Area of Nonprestressed Steel (A_s)	M^2	0.002048	Midspan
Modulus of Prestressed Steel (E_p)	$10^3 \times$MPa	195	
Modulus of Nonprestressed Steel (E_s)	$10^3 \times$MPa	210	
Modulus of HSC ($E_{c,70}$)	$10^3 \times$MPa	47.7	Adding second extra load
Modulus of HPC ($E_{c,70}$)	$10^3 \times$MPa	47.8	
Initial Stress of Prestressed Steel Immediately after Stretching (σ_{con})	MPa	1350	End

EXPERIMENTAL RESULTS AND DISCUSSION

When prestressed steels are stretched the difference of stresses between bottom fiber and top fiber at midspan is approximately 8MPa (whole section in compression) while the difference of stresses reduces to 3MPa approximately after adding second extra load(also whole section in compression). The changes of temperature, humidity, creep, shrinkage and camber are presented in Fig.3 ~ Fig.6. Data adopted in figures are mean values.

Observing Fig.3 ~ Fig.6, we can draw following conclusions:

(1). Increments of creep and camber in HPC beam are much less than that in HSC beam when the difference of tresses between bottom fiber and top fiber is large (Fig.4). Just before applying second extra load the ratio of incremental creeps between HPC beam and HSC beam is 0.685:1 (Fig.4), while the ratio of incremental cambers is 0.746:1 (Fig.5), which means that restraint effect of steel to camber increment is different from restraint effect of steel to concrete strain increment.

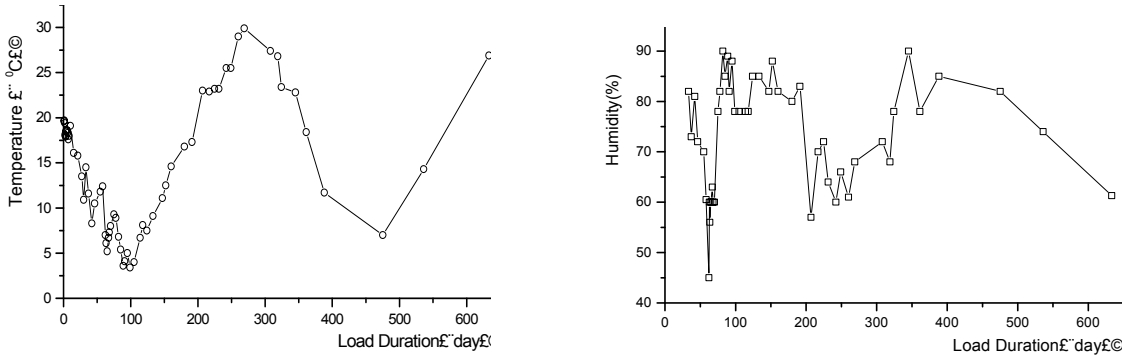

Fig.3(a) Ambient Temperature Versu Time

Fig.3(b) Ambient Humidity Versus Time

Fig.3 Ambient Temperature and Humidity

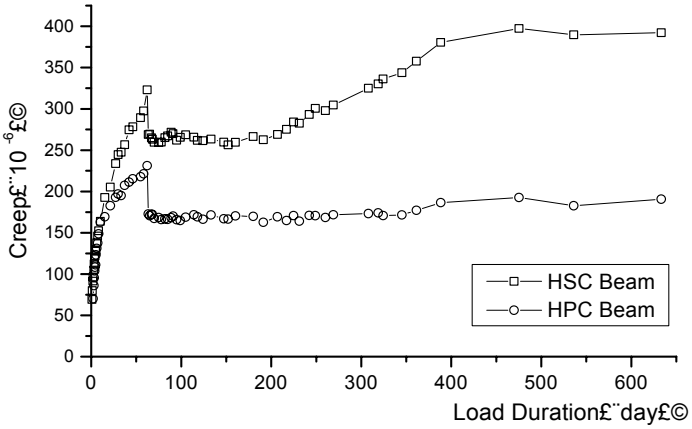

Fig. 4Time-dependent Creeps of Bottom Fiber at Midspan

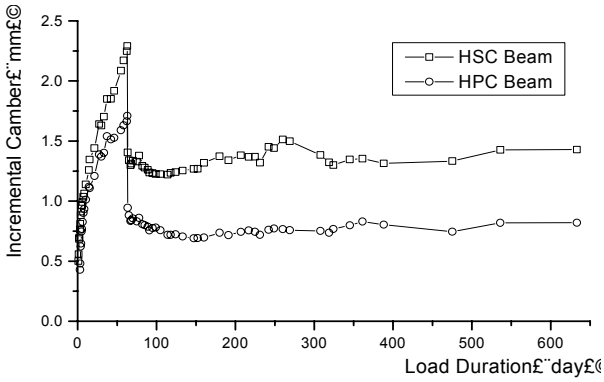

Fig.5 Time-dependent Cambers at Midspan

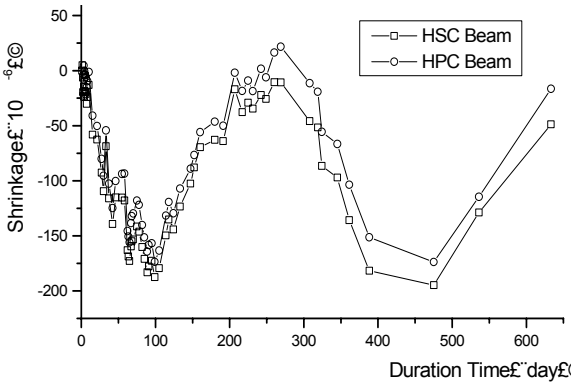

Fig.6 Time-dependent Shrinkage

(2). After applying second extra load the difference of stresses in section reduces, increment of creep in HPC beam is still much less than that in HSC beam while their camber increments almost keep same, which means camber increment is not linear to creep increment.

(3). From Fig.4 and Fig.5 we also can find that, lowering the difference of tresses in section will greatly reduce increment of camber both in HPC beam and HSC beam, although increment of creep in HSC beam still keeps in a large value.

(4). The effect of ambient humidity and temperature to creep and camber both in HPC beam and HSC beam is similar, creep and camber will increase if relative humidity reduces or temperature goes up, and the effect in HSC beam is more sensitive than in HPC beam.

(5). Longitudinal shrinkages in B1 (HPC beam) and B5 (HSC beam), including the effect of humidity and temperature, show similar characteristics (Fig.6), and the difference of shrinkages between B1 and B5 fluctuates in a range of 30×10^{-6}.

SIMPLIFIED ANALYSIS

Numerous methods, which can be divided into two groups as sophisticated analysis and simplified analysis, have been developed to calculate time-dependent effects due to creep and shrinkage in prestressed concrete members. Sophisticated analysis includes several methods accompanied with or without finite element methods[3–5], such as step-by-step method[6,7] (time-step), iterative method[8–10] and others[11,12], and many of them can only be carried out on computer[3–5,8–10]. For simplified analysis, most of the methods calculate incremental strain and deflection by considering influence coefficient due to restriction of steel[13,14]. Because of simplicity and convenience, simplified analysis has found its extensive application both in design and research, a group of formula for simplified time-dependent effect analysis are provided in this paper.

Typical prestresssed sectional properties is shown in Fig.7, where A_p is the area of prestressed steel, $A_s = A_{s1} + A_{s2}$ is the area of nonprestressed steel; e is the distance from centroid of concrete section to centroid of gravity of total steel (prestressed steel and

nonprestressed steel); $r = 1 + \sqrt{I_c / A_c}$ is radius of gyration, $\rho = 1 + e^2 / r^2$ and $\beta = e / r^2$.

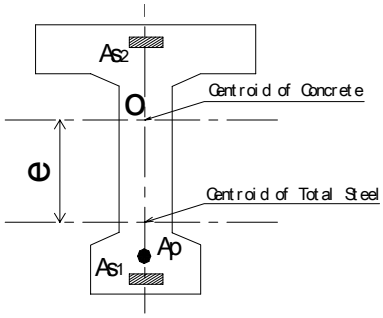

Fig.7 Steel Arrangement in Cross Section

Restraint influence coefficient can be divided into three kinds defined as below:

$$\kappa_{s,cr}(t,t_0) = \frac{\varepsilon_{b,cr}(t,t_0)}{\varphi(t,t_0)\varepsilon(t_0)} \quad , \qquad \kappa_{s,sh}(t,t_0) = \frac{\varepsilon_{b,sh}(t,t_0)}{\varepsilon_{sh}(t,t_0)} \tag{1}$$

$$\lambda_{s,cr}(t,t_0) = \frac{\phi_{b,cr}(t,t_0)}{\varphi(t,t_0)\phi(t_0)} \quad , \qquad \lambda_{s,sh}(t,t_0) = \frac{\phi_{b,sh}(t,t_0)}{\varepsilon_{sh}(t,t_0)\phi(t_0)} \tag{2}$$

$$\zeta_{s,cr}(t,t_0) = \frac{f_{b,cr}(t,t_0)}{\varphi(t,t_0)f(t_0)} \quad , \qquad \zeta_{s,sh}(t,t_0) = \frac{f_{b,sh}(t,t_0)}{\varepsilon_{sh}(t,t_0)f(t_0)} \tag{3}$$

where subscripts cr and sh represent creep and shrinkage, respectively; subscript b means the value is occurred in practical member; κ, λ, ζ represent restraint influence coefficients of steel to incremental strain, to incremental curvature and to incremental deflection, respectively; $\varepsilon(t_0)$, $\phi(t_0)$, $f(t_0)$ are elastic strain of concrete at the centroid of the gravity of steel, elastic curvature and elastic deflection at midspan due to load applied at time t_0, respectively.

EXPRESSIONS OF $\lambda_{s,cr}(t,t_0)$, $\lambda_{s,sh}(t,t_0)$, $\xi_{s,cr}(t,t_0)$, $\xi_{s,sh}(t,t_0)$ AND CAMBER CALCULATION

The maximum deflection at midspan of any prestressed concrete member at any time can be calculated from curvatures[12]

$$f_C(t) = \frac{l^2}{96}[\phi_A(t) + 10\phi_C(t) + \phi_B(t)] \tag{4}$$

where subscripts A and B are supports and C is center point of span; $f(t)$ is curvatures at relative point at time t, respectively; L is the length of span. This equation is exact when the variation of curvature is parabolic or uniformly load acts on simply supported beam.

From Eq.(2) to Eq.(4) we obtain Eq.(5) to calculate incremental deflection produced by creep and shrinkage at any time t due to load applied at time t_0

$$\Delta f_M(t,t_0) = \left[\zeta_{s,cr}(t,t_0)\varphi(t,t_0) + \zeta_{s,sh}(t,t_0)\varepsilon_{sh}(t,t_0)\right] f(t_0) \tag{5}$$

where

$$z_{s,cr}(t,t_0)=\frac{l^{A}_{s,cr}(t,t_0)f_{A}(t_0)+10l^{C}_{s,cr}f_{C}(t_0)+l^{B}_{s,cr}f_{B}(t_0)}{f_{A}(t_0)+10f_{C}(t_0)+f_{B}(t_0)} \tag{6}$$

$$z_{s,sh}(t,t_0)=\frac{l^{A}_{s,sh}(t,t_0)f_{A}(t_0)+10l^{C}_{s,sh}f_{C}(t_0)+l^{B}_{s,sh}f_{B}(t_0)}{f_{A}(t_0)+10f_{C}(t_0)+f_{B}(t_0)} \tag{7}$$

in which superscripts A, B and C refer to relative point of curvature, and

$$\begin{aligned}\lambda_{s,cr}(t,t_0)=1-\beta\ &\frac{\varepsilon_c(t_0)}{\phi(t_0)}\cdot\frac{(\mu_s n_s+\mu_p n_p)[1+\chi(t,t_0)\varphi(t,t_0)]}{1+\rho(\mu_s n_s+\mu_p n_p)[1+\chi(t,t_0)\varphi(t,t_0)]}\\ &-\beta\ \frac{\rho\zeta(t,t_0)\sigma_r(t,t_0)\mu_p[1+\chi(t,t_0)\varphi(t,t_0)]}{\phi(t_0)\varphi(t,t_0)E_c}\\ &+\beta\ \frac{n\mu}{\phi(t_0)E_c\varphi(t,t_0)}\cdot\frac{\zeta(t,t_0)\sigma_r(t,t_0)\mu_p}{1+\rho(\mu_s n_s+\mu_p n_p)[1+\chi(t,t_0)\varphi(t,t_0)]}\end{aligned} \tag{8}$$

$$l_{s,sh}(t,t_0)=-\frac{b}{f(t_0)}\times\frac{(m_s n_s+m_p n_p)[1+c(t,t_0)j(t,t_0)]}{1+r(m_s n_s+m_p n_p)[1+c(t,t_0)j(t,t_0)]} \tag{9}$$

where $\mu_s=A_s/A_c$ and $\mu_p=A_p/A_c$ are nonprestressed steel ratio and prestressed steel ratio, respectively; $n_s=\mathrm{E}_s/\mathrm{E}_c$ and $n_p=\mathrm{E}_p/\mathrm{E}_c$ are modulus ratio, E_s, E_p and E_c are modulus of nonprestressed steel, prestressed steel and concrete, respectively; $\chi(t,t_0)$ is aging coefficient which can be evaluated by equation[15]; $\sigma_r(t,t_0)$ and $\zeta(t,,t_0)$ are intrinsic steel relaxation and relaxation reduction coefficient due to creep and shrinkage, respectively, which can be calculated by equations[16].

For free end of member, incremental curvature is only produced due to shrinkage, Eq.(9) becomes

$$\lambda_{c,sh}=-\beta\frac{\mu_s n_s+\mu_p n_p}{\phi_0[1+\rho(\mu_s n_s+\mu_p n_p)]} \tag{10}$$

For calculating long-tern effect, long-term restraint influence coefficient can be evaluated by

$$l_{s,cr}(t,t_0)=1-b\frac{e_c(t_0)}{f(t_0)}\left\{\frac{nm[1+0.82j(¥,t_0)]}{1+nmr[1+0.82j(¥,t_0)]}+\frac{0.75ra_s m_p[1+0.82j(¥,t_0)]}{j(¥,t_0)}\right\} \tag{11}$$

$$\lambda_{s,sh}(t,t_0)=-\beta\frac{n\mu[1+0.8\varphi(\infty,t_0)]}{\phi_0\{1+n\mu\rho[1+0.8\varphi(\infty,t_0)]\}} \tag{12}$$

where $\mu_s+\mu_p=\mu$, $n=(n_s+n_p)/2$; $\alpha_\sigma=\sigma_r(\infty,t_0)/\sigma(t_0)$ is a stress ratio of the intrinsic steel relaxation at time infinity to elastic stress of concrete at the center point of gravity of steel (α_σ is commonly in a range of 4 ~ 7 for a compressive strength 30MPa ~ 60MPa of concrete while using prestressed strands).

From Eq.(5) ~ Eq.(12) we can calculate time-dependent deflection or long-term deflection at midspan due to creep and shrinkage based on restraint influence coefficient of

steel to incremental curvature.

EXPRESSIONS OF $k_{s,cr}(t,t_0)$, $k_{s,sh}(t,t_0)$ AND STRAIN, STRESS CALCULATION

The total strain of concrete at the centroid of gravity of steel at any time t due to load applied at time t_0 can be calculated from Eq.(13)

$$\varepsilon(t,t_0)=\frac{\sigma(t_0)}{E_c}\left[1+\kappa_{s,cr}(t,t_0)\varphi(t,t_0)\right]+\kappa_{s,sh}(t,t_0)\varepsilon_{sh}(t,t_0)+\alpha_e\cdot\Delta\mathrm{T}(t,t_0) \tag{13}$$

where $k_{s,cr}(t,t_0)$ and $k_{s,sh}(t,t_0)$ are restraint influence coefficients of steel to incremental strain due to creep and shrinkage, respectively; $\alpha_e=(\alpha_s+\mu\, n\alpha_c)/(1+\mu\, n)$ is sectional equivalent coefficient of linear expansion, α_s and α_c are coefficients of linear expansion of steel and concrete, respectively; $\varepsilon_{sh}(t,t_0)$ is free shrinkage of concrete; $\Delta\mathrm{T}(t,t_0)$ is the change of temperature from time t_0 to t.

$k_{s,cr}(t,t_0)$ and $k_{s,sh}(t,t_0)$ can be calculated as below

$$k_{s,cr}(t,t_0)=\frac{1}{1+\rho(\mu_s n_s+\mu_p n_p)\left[1+\chi(t,t_0)\varphi(t,t_0)\right]}$$

$$-\frac{\sigma_r(t,t_0)}{\sigma(t_0)\varphi(t,t_0)}\cdot\frac{\mu_p\rho\zeta(t,t_0)\left[1+\chi(t,t_0)\varphi(t,t_0)\right]}{1+\rho(\mu_s n_s+\mu_p n_p)\left[1+\chi(t,t_0)\varphi(t,t_0)\right]} \tag{14}$$

$$\kappa_{s,sh}(t,t_0)=-\frac{1}{1+\rho(\mu_s n_s+\mu_p n_p)\left[1+\chi(t,t_0)\varphi(t,t_0)\right]} \tag{15}$$

For calculating long-tern effect, long-term influent coefficients can be evaluated by

$$k_{s,cr}(\infty,t_0)=\frac{1}{1+n\rho\mu\left[1+0.82\varphi(\infty,t_0)\right]}\left(1-\alpha_\sigma\rho\;\mu_p\left[0.6+\frac{0.82}{\varphi(\infty,t_0)}\right]\right) \tag{16}$$

$$\kappa_{s,sh}(\infty,t_0)=-\frac{1}{1+n\mu\rho\left[1+0.82\varphi(\infty,t_0)\right]} \tag{17}$$

The stress of concrete at the center of gravity of steel at any time t due to load applied at time t_0 can be calculated from Eq.(18)

$$\sigma_c(t,t_0)=\sigma_c(t_0)-\frac{\sigma_c(t_0)\varphi(t,t_0)\left[1-k_{s,cr}(t,t_0)\right]+E_c\varepsilon_{sh}(t,t_0)\left[1-k_{s,sh}(t,t_0)\right]}{1+\chi(t,t_0)\varphi(t,t_0)} \tag{18}$$

This equation shows that the time-dependent stress of concrete will be reduced due to creep and shrinkage, and the reducing progress is accelerated by restraint of steel. As time

$t(> t_0)$ increases, the rate of creep and shrinkage will slow down while the restraint of steel to creep and shrinkage will heighten (as shown in Fig.9), thus redistribution of stresses between concrete and steel will intensify by reducing stress of concrete and increasing the stress of steel.

DISCUSSION ON RESTRAINT INFLUENCE COEFFICIENTS

If $\mu_s = \mu_p = 0$, from Eq.(8), Eq.(9), Eq.(14) and Eq.(15) we have $\lambda_{s,cr}(t,t_0) = 1$, $\lambda_{s,sh}(t,t_0) = 0$, $\kappa_{s,cr}(t,t_0) = 1$ and $\kappa_{s,sh}(t,t_0) = 0$ which means no restraint of steel occurs; If $\mu_s \neq 0$ and $\mu_p = 0$, Eq.(8) becomes

$$\lambda_{s,cr}(t,t_0) = 1 - \beta \frac{\varepsilon_c(t_0)}{\phi(t_0)} \cdot \frac{n_s \mu_s [1 + \chi(t,t_0)\varphi(t,t_0)]}{1 + \rho\, n_s \mu_s [1 + \chi(t,t_0)\varphi(t,t_0)]} \tag{8a}$$

$$k_{s,cr}(t,t_0) = \frac{1}{1 + n_s \mu_s \rho\, [1 + \chi(t,t_0)\varphi(t,t_0)]} \tag{14a}$$

These equations can be used to calculate time-dependent effect due to creep and shrinkage in fully compressed reinforcement section, typical member in such condition is reinforcement concrete column.

The following is mainly to discuss restraint influence coefficient relating to creep. The adopted parameters come from tested beam and elastic variables come from experimental data. The modified models of creep and shrinkage given in CEB-FIB Model Code 1990 (MC90) are used by fitting data deduced from strains of tested beam[17].

Eq.(8) shows that $\lambda_{s,cr}(t,t_0)$ is not a constant which depends on steel ratio, steel arrangement, steel relaxation, creep coefficient, concrete modus , elastic strain and stress of concrete and elastic curvature. For $\lambda_{s,cr}(t,t_0)$ given in reference 13 (Eq.8b), the main factor affecting $\lambda_{s,cr}(t,t_0)$ is steel ratio of compressive reinforcement and tensile reinforcement, respectively; as reference 12, 14 point out, it's impossible to calculate deflection accurately only considering steel ratio. Also, Eq.(8) is different from equation provided in reference 13 (Eq.6), which ignores the effect of elastic ratio $\varepsilon_c(t_0)/\phi(t_0)$ that plays an important role in curvature increment, i.e., the influence of steel to curvature disappears if $\phi(t_0)$ is infinity (elastic deflection is zero), even though strain of concrete is in a large value; anymore, equation in reference 14 ignores the steel relaxation which reduces deflection increment unneglectable due to creep and shrinkage.

Fig.8 and Fig.9 draw out the time-dependent $\lambda_{s,cr}(t,t_0)$ and $\kappa_{s,cr}(t,t_0)$, respectively. In figures, the effects due to different load applied time t_0 ($t_0 = 10d$ and $t_0 = 70d$, t_0 is age of concrete) both in HSC beam and HPC beam are compared.

Fig.8 and Fig.9 show following characteristics:

(1). As time $t(> t_0)$ increases, both rate and value of $\lambda_{s,cr}(t,t_0)$ and $\kappa_{s,cr}(t,t_0)$ slow down which means the restraint of steel to creep enhances, so it is very important to analyze the early creep effect with a time-dependent influence coefficient in some cases, i.e., for prestressed concrete bridges fabricated in cantilevered construction method.

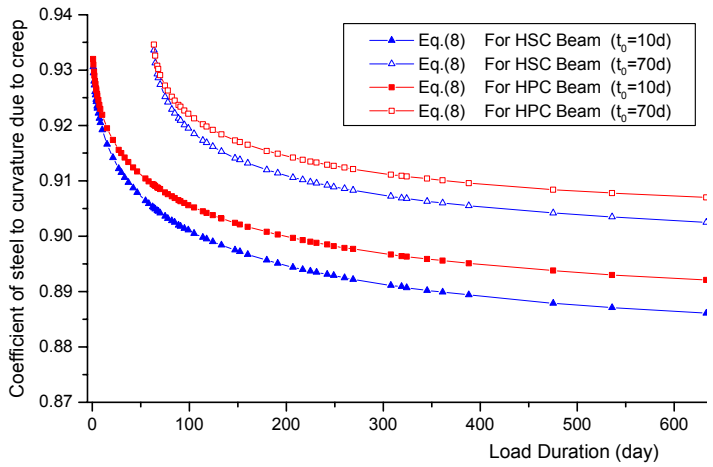

Fig.8 Time-dependent Influence Coefficient of Steel to Curvature Increment Due to Creep

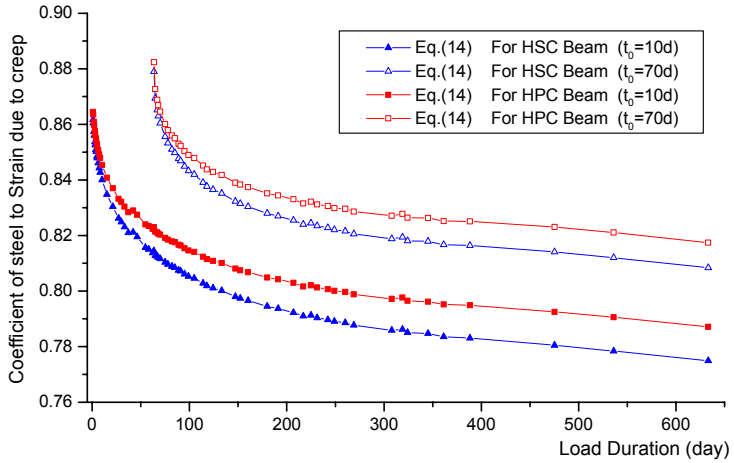

Fig.9 Time-dependent Influence Coefficient of Steel to Strain Increment Due to Creep

(2). $\lambda_{s,cr}(t,t_0)$ and $\kappa_{s,cr}(t,t_0)$ are different for HSC beam and HPC beam, even the applied load time is same, and the difference will enlarge as time passes, which means different kinds of concrete members(even have same mechanical behavior of concrete and sectional properties) hold different $\lambda_{s,cr}(t,t_0)$ and $\kappa_{s,cr}(t,t_0)$.

(3). $\lambda_{s,cr}(t,t_0)$ and $\kappa_{s,cr}(t,t_0)$ are different in the same beam if load applied time is different. The earlier the load is applied, the larger the influence coefficients will have, which means the restraint of steel to creep will be relatively small for old concrete.

The ratio of time-dependent influence coefficient to long-term influence coefficient is listed in Table 4., in which we can see that the long-term influence coefficient always reduces over10 percent comparing to initial influence coefficient when the load is applied. It is necessary to use time-dependent influence coefficients to analyze time-dependent effect.

Table 4 Comparison of Restraint Influence Coefficient

	$t_0 = 10d$	$t_1 = 70d$
HSC Beam	$k_{s,cr}(10.5d,t_0) : k_{s,cr}(20y,t_0) = 1 : 0.836$	$k_{s,cr}(70.5d,t_1) : k_{s,cr}(20y,t_1) = 1 : 0.869$
	$\lambda_{s,cr}(10.5d,t_0) : \lambda_{s,cr}(20y,t_0) = 1 : 0.841$	$\lambda_{s,cr}(70.5d,t_1) : \lambda_{s,cr}(20y,t_1) = 1 : 0.873$
HPC Beam	$k_{s,cr}(10.5d,t_0) : k_{s,cr}(20y,t_0) = 1 : 0.848$	$k_{s,cr}(70.5d,t_0) : k_{s,cr}(20y,t_1) = 1 : 0.875$
	$\lambda_{s,cr}(10.5d,t_0) : \lambda_{s,cr}(20y,t_0) = 1 : 0.855$	$\lambda_{s,cr}(70.5d,t_1) : \lambda_{s,cr}(20y,t_1) = 1 : 0.881$
Note: "d" represents "day, "y" represents "year".		

COMPARISON OF THEORETICAL RESULTS TO EXPERIMENTAL DATA

Before applying second extra load, the difference of stresses between top fiber and bottom fiber in section is relatively large and the incremental cambers and strains increase fast, so it's better to compare theoretical values, based on this paper's formulae, with experimental data before applying second extra load. Theoretical values and experimental results of creep and incremental camber due to creep and shrinkage both in HSC beam and HPC beam, respectively, are plotted in Fig.10, Fig.11. From theses two figures we can see that theoretical values fit well with experimental results.

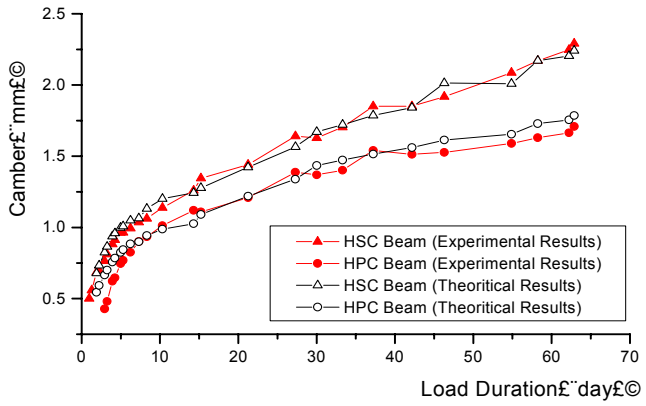

Fig.10 Comparison of Time-dependent Camber

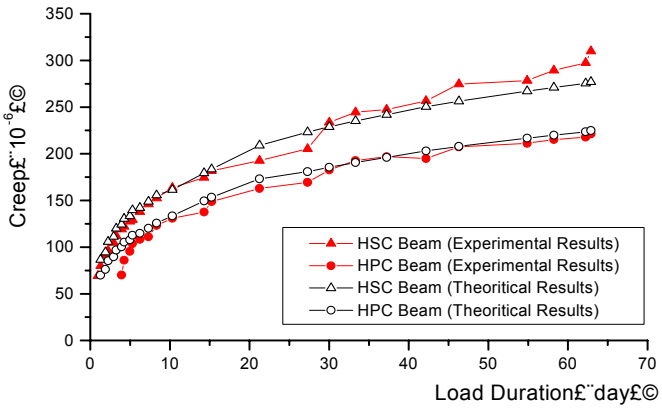

Fig.11 Comparison of Creep

CONCLUDING REMARKS

Over 600 days comparative experiment on time-dependent behavior due to creep and shrinkage in prestressed concrete members has been finished. Experimental results show that creep and incremental camber are much less in HPC500 beam than that in HSC500 beam, and difference of stresses between top fiber and bottom fiber in section makes important effect on reducing long-term camber. These will be helpful to understand and adopt methods to control long-term camber, and the reliable experimental data will be useful to practical engineering design.

Based on concept of restraint influence coefficient of steel to creep and shrinkage effect, a simplified analysis on time-dependent behavior in prestressed concrete members is given. Discussion on restraint influence coefficients shows that coefficients are time-dependent variables and depend on many aspects. Different load applied times in the same member bear different values of coefficients, concretes with different characteristics of creep and shrinkage (even with same mechanical behavior) also hold different values of coefficients, and it should be mentioned that elastic curvature plays an important role in restraint influence coefficient of steel to curvature increment and camber increment. Results of theoretical analysis agree reasonably well with the measured increments of strain and camber.

REFERENCES

1. Ghali, A., “Stress and Strain Analysis in Prestressed Concrete: A critical Review”, *PCI Journal*, Nov.-Dec.,1989, pp.80-97.
2. Bažant Z P., “Prediction of concrete creep effects using age-adjusted effective modulus method”, *ACI Journal , proceedings*, V.69, N.4, Apr. 1972, pp.212-217
3. Roca,P., and Marí,A.R.,“Numerical Treatment of Prestressing Tendons in The Nonlinear of Prestressed Concrete Structures”, *Comp.and Struct.*, 1993, V.46, N.5 , pp.905-916.

4. Buragohain, D.N. and Sisshaye, V.R., "Finit Element Analysis of Prestressed Concrete Box Bridges", *Journal of Structural Engineering*, V.24, N.3, Oct.1997, pp.135-141
5. Van Greunen, Johannes, Scordelis, Alexander C., "Nonlinear Analysis of Prestressed Concrete Slabs", *Journal of Structural Engineering*, , V.109, N.7, Jul.1983 pp.1742-1760.
6. Herbert, T.J., "Computer Analysis of Deflections and Stresses in Stage Constructed Concrete Bridges", *PCI Journal*, V.35, N.3, May-Jun.1990, pp.52-63.
7. Gutiérrez, S.E., Cudmani, R.O. and Danesi, R.F., "Time-Dependent Analysis of Reinforced and Prestressed Concrete Members", *ACI Structural Journal*, Jul.-Aug. 1996,V.93, N.4, pp.420-427.
8. Prasada Rao, A.S., "Direct Analysis of Prestressed Concrete Members", *Journal of Structural Engineering*, V.116, N.12, Dec.1989, pp.3432-3447.
9. Moustafa, S.E., "Nonlinear Analysis of Reinforced and Prestressed Concrete Members", *PCI Journal*, V.27, N.1, Sept.-Oct.1986, pp.126-143.
10. Sapountzakis, E.J. and Katsikadelis, J.T., "Analysis of Prestressed Concrete Slab-and-Beam Structures", *Computational Mechanics*, V.27,N.6,Sept. 2001, pp.492-503.
11. Dilger, Walter H.,"Creep Analysis of Prestressed Concrete Structures Using Creep -Transformed Section Properties", *PCI Journal*, V.27,N.1, Jan-Feb, 1982, pp.98-118.
12. Ghali A, Azarnejad A., "Deflection Prediction of Members of Any Concrete Strength", *ACI Structural Journal*, V.96, N.5, Sept.-Oct.1999, pp.807-816
13. Gilbert, R.I., "Deflection Calculation For Reinforced Concrete Structures-Why We Sometimes Get Wrong",*ACI Structural Journa*l,V.96,N.6,Nov.-Dec.1999, pp.1027-1032
14. Bandyopadhyay, T.K. and Sengupta, B., "Effect of Deferred Initial Loading and Percentage of Steel on Time-Dependent Losses and Deformations of Prestressed Members", *ACI Structural Journal*, V.96, N.5,1999, pp.807-816
15. Lacidogna, G. and Tarantino, M., "Approximate Expressions for the Aging Coefficient and The Relaxation Function in the Viscoelastic Analysis of Concrete Structures", *Materials and Structures*, V.29, Apr.1996, pp.131-140.
16. Ghali A, Trevino J., "Relaxation of steel in prestressed concrete", *PCI Journal*, Sept.-Oct. 1985, pp.82-94
17. Di, H. And Chen, Z.Q, "Prediction of Long-Term Effect of Creep and Shrinkage on Newly-built Prestressed Concrete Bridge Based on Short-Term Test Results", *China Railway Science*, V.24, N.3, May-Jun.2003, pp.44-49